Propagation of squeezed-light pulses in dispersive and absorbing linear dielectrics

Eduard Schmidt, Ludwig Knöll, and Dirk-Gunnar Welsch
Friedrich-Schiller-Universität Jena, Theoretisch-Physikalisches Institut, Max-Wien Platz 1, D-07743 Jena, Germany
(Received 10 January 1996)

The behavior of short quantum light pulses propagating in dispersive and absorbing linear ground-state dielectrics is studied, with special emphasis on squeezed pulses. The analysis is based on normally ordered correlation functions of the electric-field strength, which are related to quantities at the entrance plane, on using quantum Langevin equations. Using nonmonochromatic-mode expansion and restricting attention to a single-mode pulse in a squeezed state, the influence on squeezing of the pulse propagation in the medium is discussed in both the time and frequency domains, and it is shown that the noise reduction observable in homodyne detection sensitively depends on the phase control used. Effects, such as squeezing enhancement associated with pulse compression and the destructive influence of the spectral shift caused by absorption, are demonstrated. The numerical results are supplemented by analytical estimations derived for narrow-bandwidth Gaussian pulses. [S1050-2947(96)00407-6]

PACS number(s): 42.50.−p

I. INTRODUCTION

The study of propagation of quantum light pulses through dispersive and absorptive dielectric matter has been a subject of increasing interest. Apart from more fundamental problems, such as the determination of multilayer dielectric-barrier traversal times of photons [1–4], there have been a number of open questions that are closely related to practical applications, such as low-noise optical communication systems. It is well known that the transmission of information through fibers by means of optical pulses requires detailed knowledge of the influence of the medium properties on the radiation [5]. In particular, linear dispersion and absorption as well as nonlinear optical properties of the medium may drastically affect the pulse properties.

Although a number of effects can be understood, in principle, from classical optics [6], quantum light pulses give rise to typical nonclassical features whose explanation requires additional considerations. It is well known that light exhibiting nonclassical properties, such as squeezing, antibunching, or sub-Poissonian statistics, reacts very sensitively to perturbations and the noise associated with them. The propagation of quantized light through dielectric matter has been studied under various aspects. In particular, the action of a wide class of passive optical instruments can be explained by using the model of macroscopic dielectric bodies (see, e.g., [7]). Further, photon tunneling through multilayer dielectric mirrors, dispersion cancellation in two-photon interferences, and related nonlocal effects have been considered [2–4,8–11]. Other interesting examples are spontaneous emission [12] and propagation of continuous-wave squeezed light [13] in dielectric media. In the nonlinear optical regime the generation and propagation of squeezed quantum solitons has been of particular interest [14–17]. The use of squeezed soliton pulses in optical communication systems could offer novel possibilities in order to improve the performance of such systems, because of the low-noise properties of the pulses [17].

There have been various approaches to the problem of quantization of radiation in linear dielectric media. Quantization schemes have been developed for radiation in homogeneous and inhomogeneous dispersionless dielectric matter and homogeneous dispersive dielectrics [18–23], and extensions to nonlinear media have been given [14–16,21,24]. In order to describe the long-distance behavior of short quantum light pulses, a quantization scheme is desired that is consistent with the Kramers-Kronig relations and hence allows for both dispersion and absorption. The problem has been considered in a number of papers [25–34]. In particular, the method of Green-function expansion developed in [34] enables one to include dispersion and absorption in the theory and systematically treat both homogeneous and inhomogeneous dielectric matter.

Using the concepts developed in [13,34], in the present paper we study the propagation of short quantum light pulses in dispersive and absorptive linear dielectrics, with special emphasis on squeezed light pulses, the pulses being analyzed in terms of so-called nonmonochromatic modes [35,36]. Restricting attention to the dielectric-matter ground state, expressions for the normally ordered correlation functions of the electric-field strength are given. The theory is used to study the space-time evolution of the electric-field strength noise of a quantum pulse that at the entrance plane is assumed to be in a squeezed single-mode quantum state. It is shown that the electric-field strength variance observed in homodyne detection sensitively depends on the local-oscillator frequency and phase control chosen. Assuming a single medium resonance and a Gaussian spectral shape of the incoming pulse, both numerical and analytical results are presented and the influence of dispersion and absorption on the observed electric-field strength variance of the pulse is discussed. In particular, it is shown that effects, such as pulse broadening and compression, well known from classical optics may also be observed in the squeezing behavior of the pulse. Conditions for preserving the squeezing effect in long-distance propagation are derived.

The paper is organized as follows. In Sec. II the quantization scheme is outlined. The space-time evolution of the quantum-statistical properties of light pulses is described in terms of normally ordered correlation functions of the

electric-field strength, which are expressed in terms of normally ordered moments of the photonic creation and destruction operators associated with the nonmonochromatic modes of the pulse at the entrance plane. In Sec. III the theory is applied to pulses that enter the medium in a squeezed single-mode state, and an analysis of the development of the electric-field noise in the further course of pulse propagation is given, with special emphasis on homodyne detection. Finally, a summary and some concluding remarks are given in Sec. IV.

II. FUNDAMENTALS

A. Quantization scheme

Let us consider linearly polarized radiation propagating in the positive x direction in a linear dielectric whose permittivity

$$\varepsilon(\omega)=\varepsilon_r(\omega)+i\varepsilon_i(\omega) \tag{1}$$

is a complex function of frequency ω. It is well known that $\varepsilon_r(\omega)$ and $\varepsilon_i(\omega)$ describing the effects of dispersion and absorption, respectively, are related to each other by the Kramers-Kronig relations, because of causality. Introducing the (Heisenberg) operator of the electric-field strength,

$$\hat{E}(x,t)=\hat{E}^{(+)}(x,t)+\hat{E}^{(-)}(x,t), \tag{2}$$

$$\hat{E}^{(-)}(x,t)=[\hat{E}^{(+)}(x,t)]^{\dagger}, \tag{3}$$

where $\hat{E}^{(+)}(x,t)$ and $\hat{E}^{(-)}(x,t)$, respectively, are the positive and negative frequency parts, and following Refs. [13,34] we may represent $\hat{E}^{(+)}(x,t)$ as

$$\hat{E}^{(+)}(x,t)=\int_0^{\infty} d\omega\, K(\omega)e^{-i\omega t}e^{ik_r(\omega)x}\hat{a}(x,\omega), \tag{4}$$

where the abbreviation

$$K(\omega)=i\sqrt{\frac{\hbar\omega}{4\pi c n_r(\omega)\varepsilon_0\mathcal{A}}}\frac{n_r(\omega)}{n(\omega)} \tag{5}$$

has been used. Here and in the following, $n(\omega)$ and $k(\omega)$, respectively, are the complex refractive index and wave number,

$$n(\omega)=n_r(\omega)+in_i(\omega)=\sqrt{\varepsilon(\omega)}, \tag{6}$$

$$k(\omega)=k_r(\omega)+ik_i(\omega)=\frac{\omega}{c}n(\omega), \tag{7}$$

and $\mathcal{A}$ is the normalization area perpendicular to the x direction. Equation (2) together with Eqs. (3) and (4) may be regarded as a generalized mode expansion of the electric field, where, owing to the propagation-assisted damping of the waves, the amplitude operators $\hat{a}(x,\omega)$ and $\hat{a}^{\dagger}(x,\omega)$ depend on x. They satisfy the commutation relation

$$[\hat{a}(x,\omega),\hat{a}^{\dagger}(x',\omega')]=e^{-k_i(\omega)|x-x'|}\delta(\omega-\omega') \tag{8}$$

and obey quantum Langevin equations, so that $\hat{a}(x,\omega)$ can easily be related to $\hat{a}(x',\omega)$, $x\geqslant x'$, as

$$\hat{a}(x,\omega)=e^{-k_i(\omega)(x-x')}\hat{a}(x',\omega) - i\sqrt{2k_i(\omega)}\int_{x'}^{x}dy\, e^{-k_i(\omega)(x-y)}e^{-ik_r(\omega)y}\hat{f}(y,\omega), \tag{9}$$

where $-i\sqrt{2k_i(\omega)}e^{-ik_r(\omega)y}\ \hat{f}(y,\omega)$ plays the role of a Langevin operator noise source. Note that when ω is far from the medium resonances, so that the damping may be disregarded, $\varepsilon_i(\omega)\to 0$, ordinary mode expansion is recognized. The operators $\hat{a}(x,\omega)$ and $\hat{a}^{\dagger}(x,\omega)$ become independent of x, $\hat{a}(x,\omega),\hat{a}^{\dagger}(x,\omega)\to\hat{a}(\omega),\hat{a}^{\dagger}(\omega)$, where $\hat{a}(\omega)$ and $\hat{a}^{\dagger}(\omega)$ are the well-known photon destruction and creation operators. It is worth noting that when in the frequency interval under consideration the losses are sufficiently small so that $n_r(\omega)/n(\omega)\approx 1$ in Eq. (5), the form of the electric-field operator given above agrees with that derived in Ref. [31], where the scattering centers that cause the losses in the medium are modeled by beam splitters.

B. Radiation-field correlation functions

The study of the quantum statistics of radiation is frequently based on an analysis of normally ordered electric-field strength correlation functions available from measurements. Let us therefore consider correlation functions of the type

$$C^{(m,n)}(\{x_\mu,t_\mu\})=\left\langle\left[\prod_{\mu=1}^{m}\hat{E}^{(-)}(x_\mu,t_\mu)\right]\times\left[\prod_{\mu=m+1}^{m+n}\hat{E}^{(+)}(x_\mu,t_\mu)\right]\right\rangle \tag{10}$$

and suppose that the radiation is known at a certain entrance plane (in the following $x=0$). Further, we assume that the temperature is sufficiently low, so that the dielectric matter does not act (in the optical frequency domain) as a thermal light source. Using Eqs. (2)–(4) and (9), we easily see that in the case under study Eq. (10) may be rewritten as

$$C^{(m,n)}(\{x_\mu,t_\mu\})=\int_0^{\infty}d\omega_1 K^*(\omega_1)\exp[-ik^*(\omega_1)x_1+i\omega_1 t_1]\cdots\int_0^{\infty}d\omega_{m+n}K(\omega_{m+n}) \times\exp[ik(\omega_{m+n})x_{m+n}-i\omega_{m+n}t_{m+n}]\underline{C}^{(m,n)}(\{\omega_\mu\}), \tag{11}$$

where

$$\underline{C}^{(m,n)}(\{\omega_\mu\})=\left\langle\left[\prod_{\mu=1}^{m}\hat{a}^\dagger(\omega_\mu)\right]\left[\prod_{\mu=m+1}^{m+n}\hat{a}(\omega_\mu)\right]\right\rangle. \tag{12}$$

Here, the operators $\hat{a}(\omega_\mu)\equiv\hat{a}(x=0,\omega_\mu)$ and $\hat{a}^\dagger(\omega_\mu)\equiv\hat{a}^\dagger(x=0,\omega_\mu)$ that satisfy the familiar bosonic commutation relation

$$[\hat{a}(\omega),\hat{a}^\dagger(\omega')]=\delta(\omega-\omega') \tag{13}$$

[cf. Eq. (8), with $x=x'$] may be regarded as the photon creation and destruction operators associated with the monochromatic modes of the incoming radiation.

With regard to the study of light pulses, it may be useful to introduce photons associated with other than monochromatic waves [35,36], viz.,

$$\hat{c}_j=\int_0^\infty d\omega\ \eta_j^*(\omega)\hat{a}(\omega), \tag{14}$$

where the $\eta_j(\omega)$ are an orthonormal and complete set of functions in the ω domain, so that $\hat{c}_j$ and $\hat{c}_j^\dagger$ satisfy the bosonic commutation relation

$$[\hat{c}_j,\hat{c}_{j'}^\dagger]=\delta_{jj'}. \tag{15}$$

Inverting Eq. (14),

$$\hat{a}(\omega)=\sum_j\ \eta_j(\omega)\hat{c}_j, \tag{16}$$

and combining Eqs. (12) and (16), we find that

$$\underline{C}^{(m,n)}(\{\omega_\mu\})=\sum_{\{j_\mu\}}\left[\prod_{\mu=1}^{m}\eta_{j_\mu}^*(\omega_\mu)\right]\times\left[\prod_{\mu=m+1}^{m+n}\eta_{j_\mu}(\omega_\mu)\right]\Gamma_{\{j_\mu\}}^{(m,n)}, \tag{17}$$

where

$$\Gamma_{\{j_\mu\}}^{(m,n)}=\left\langle\left[\prod_{\mu=1}^{m}\hat{c}_{j_\mu}^\dagger\right]\left[\prod_{\mu=m+1}^{m+n}\hat{c}_{j_\mu}\right]\right\rangle. \tag{18}$$

III. SQUEEZED SINGLE-MODE PULSE PROPAGATION

A. Basic equations

To illustrate typical effects of dispersion and absorption on the quantum statistics of short nonclassical light pulses propagating through linear dielectrics, let us restrict attention to squeezed pulses. For this purpose we consider a pulse that is generated in such a way that it effectively corresponds to one excited nonmonochromatic mode, which of course consists of a continuum of excited monochromatic modes. In this case the sums in Eq. (17) reduce to one term, that is to say,

$$\underline{C}^{(m,n)}(\{\omega_\mu\})=\left[\prod_{\mu=1}^{m}\eta^*(\omega_\mu)\right]\left[\prod_{\mu=m+1}^{m+n}\eta(\omega_\mu)\right]\langle(\hat{c}^\dagger)^m\hat{c}^n\rangle, \tag{19}$$

where for notational convenience the mode subscript has been omitted. Hence, Eq. (11) reads as

$$C^{(m,n)}(\{x_\mu,t_\mu\})=\left[\prod_{\mu=1}^{m}E^*(x_\mu,t_\mu)\right]\left[\prod_{\mu=m+1}^{m+n}E(x_\mu,t_\mu)\right]\times\langle(\hat{c}^\dagger)^m\hat{c}^n\rangle. \tag{20}$$

Here,

$$E(x,t)=\frac{1}{2\pi}\int_0^\infty d\omega\,E(x,\omega)e^{-i\omega t}, \tag{21}$$

where

$$E(x,\omega)=2\pi K(\omega)\,\eta(\omega)e^{ik(\omega)x} \tag{22}$$

may be regarded as the spectral function of the pulse at propagation length x, the function $\eta(\omega)$ being normalized to unity,

$$\int_0^\infty d\omega|\,\eta(\omega)|^2=1. \tag{23}$$

From Eqs. (2), (10), and (20), the average of the electric-field strength of the pulse reads as

$$\langle\hat{E}(x,t)\rangle=E(x,t)\langle\hat{c}\rangle+E^*(x,t)\langle\hat{c}^\dagger\rangle \tag{24}$$

and the pulse intensity corresponds to

$$I(x,t)\equiv\langle\hat{E}^{(-)}(x,t)\hat{E}^{(+)}(x,t)\rangle=|E(x,t)|^2\langle\hat{c}^\dagger\hat{c}\rangle. \tag{25}$$

Similarly, the normally ordered electric-field strength variance is given by

$$\langle:[\Delta\hat{E}(x,t)]^2:\rangle=2|E(x,t)|^2\langle\Delta\hat{c}^\dagger\Delta\hat{c}\rangle+\{E^2(x,t)\langle(\Delta\hat{c})^2\rangle+\text{c.c.}\}, \tag{26}$$

where the notation $\Delta\hat{O}=\hat{O}-\langle\hat{O}\rangle$ has been introduced.

Light is said to be squeezed when (at chosen space-time points) $\langle:[\Delta\hat{E}(x,t)]^2:\rangle$ attains negative values, that is to say, when the noise of the electric-field strength can be reduced below the vacuum level. Let us assume that the pulse under consideration is in a squeezed vacuum state

$$|\Psi\rangle=\hat{S}(s)|0\rangle, \tag{27}$$

where $|0\rangle$ and $\hat{S}(s)$, respectively, are the ordinary vacuum state and the squeeze operator,

$$\hat{S}(s)=\exp[-\tfrac{1}{2}s(\hat{c}^{\dagger})^2+\text{H.c.}], \tag{28}$$

the complex number

$$s=|s|e^{i\varphi_s} \tag{29}$$

being the squeeze parameter. Straightforward calculation yields (see, e.g., [7])

$$\langle\hat{c}\rangle=0, \tag{30}$$

$$\langle\Delta\hat{c}^{\dagger}\Delta\hat{c}\rangle=\langle\hat{c}^{\dagger}\hat{c}\rangle=\sinh^2|s|, \tag{31}$$

$$\langle(\Delta\hat{c})^2\rangle=\langle\hat{c}^2\rangle=-e^{i\varphi_s}\cosh|s|\sinh|s|. \tag{32}$$

Hence, from Eqs. (25) and (26) we find that

$$\langle\hat{E}(x,t)\rangle=0, \tag{33}$$

$$I(x,t)=|E(x,t)|^2\sinh^2|s|, \tag{34}$$

$$\langle:[\Delta\hat{E}(x,t)]^2:\rangle=2I(x,t)-\cosh|s|\sinh|s|\{E^2(x,t)e^{i\varphi_s}+\text{c.c.}\}. \tag{35}$$

B. Homodyne detection

It is well known that squeezing can be measured in balanced homodyne detection, where the signal field and a strong local oscillator are superimposed by a beam splitter and the interfering field is measured. In particular, when a (quasi)monochromatic local oscillator is used the electric-field strength relevant for short-time detection is given by (see, e.g., [7,37,38])

$$\hat{E}_d(x,t)=\exp[i\omega_d t+i\theta]\hat{E}^{(+)}(x,t)+\text{H.c.}, \tag{36}$$

where ω_d and θ, respectively, are the frequency and the phase of the local oscillator. Substituting in Eqs. (34) and (35) for $E(x,t)$, Eq. (21) [together with Eq. (22)], the slowly varying quantity $E_d(x,t)e^{i\theta}$, where

$$E_d(x,t)=e^{i\omega_d t}E(x,t), \tag{37}$$

the electric-field strength variance measured (during a sufficiently small time interval) reads as

$$\langle:[\Delta\hat{E}_d(x,t)]^2:\rangle=2I_d(x,t)-\cosh|s|\sinh|s|\{E_d^2(x,t)e^{i(\varphi_s+2\theta)}+\text{c.c.}\}, \tag{38}$$

$$I_d(x,t)=|E_d(x,t)|^2\sinh^2|s|=I(x,t). \tag{39}$$

From Eq. (38) we expect that the normally ordered variance of the electric-field strength, in general, sensitively depends on x and t through the phase of $E_d(x,t)$, which can drastically be changed during the propagation of the pulse in the dielectric matter. Hence, control of the noise of the electric-field strength requires careful control of the local-oscillator phase θ. When at chosen distance x from the entrance plane a time-independent phase of the local oscillator, θ_x, is used, an optimal value for θ_x may be found from the requirement that the time-integrated normally ordered electric-field strength variance

$$\langle:[\Delta\hat{E}_d(x)]^2:\rangle=\int_{-\infty}^{\infty}dt\langle:[\Delta\hat{E}_d(x,t)]^2:\rangle \tag{40}$$

(with $\langle:[\Delta\hat{E}_d(x,t)]^2:\rangle$ from Eq. (38)) is minimal, which implies that the total electric-field noise observed over the whole pulse is minimal. In this case $\varphi_s+2\theta_x$ compensates the phase of $\int_{-\infty}^{\infty}dt\,E_d^2(x,t)$,

$$\varphi_s+2\theta_x=-\arg\left[\int_{-\infty}^{\infty}dt\,E_d^2(x,t)\right], \tag{41}$$

and Eq. (40) takes the form

$$\langle:[\Delta\hat{E}_d(x)]^2:\rangle=2W(x)-2\cosh|s|\sinh|s|\left|\int_{-\infty}^{\infty}dt\,E_d^2(x,t)\right|, \tag{42}$$

where

$$W(x)=\sinh^2|s|\int_{-\infty}^{\infty}dt|E_d(x,t)|^2 \tag{43}$$

is closely related to the overall pulse energy. Clearly, the total noise detected in this scheme must not necessarily be below the vacuum level, because both noise reductions and enhancements contribute. Observation of an electric-field strength noise reduced below the vacuum level at any space-time point requires phase control that also includes time. In particular, when the phase of the local oscillator, $\theta_{x,t}$, is chosen in such a way that in Eq. (38) $\varphi_s+2\theta_{x,t}$ exactly compensates the phase of $E_d^2(x,t)$,

$$\varphi_s+2\theta_{x,t}=-\arg[E_d^2(x,t)], \tag{44}$$

then at any space-time point the minimum noise is observed, that is to say,

$$\langle:[\Delta\hat{E}_d(x,t)]^2:\rangle=2(1-\coth|s|)I_d(x,t). \tag{45}$$

It should be noted that the electric-field strength variance in Eq. (38) is based on the detection operator (36) that characterizes short-time measurements, such as the measurements studied in Ref. [38], and can advantageously be used in order to temporally resolve the properties of pulses. When the measuring time cannot be regarded as being short the detection operator is given by a time-integral over the field strength $\hat{E}_d(x,t)$ in Eq. (36). This type of detection operator has been studied in Ref. [31] for measuring narrow bandwidth radiation propagating along attenuating and amplifying optical fibers.

When in (balanced) homodyne detection the (difference) photocurrent signal is passed through a spectral filter onto the recorder, then spectral properties of the electric-field noise can be observed. In particular, integrating the spectrally filtered signal over the whole pulse yields a time-

independent squeezing spectrum $S(x,\Omega_s)$ closely related to the Fourier transform $\hat{E}_d(x,\Omega_s)$ of the electric-field strength $\hat{E}_d(x,t)$,

$$S(x,\Omega_s)=\frac{1}{2\pi}\langle:\Delta\hat{E}_d(x,\Omega_s)\Delta\hat{E}_d(x,-\Omega_s):\rangle, \quad (46)$$

where

$$\hat{E}_d(x,\Omega_s)=\int_{-\infty}^{\infty}dt\,e^{i\Omega_s t}\hat{E}_d(x,t). \quad (47)$$

An explicit expression for $S(x,\Omega_s)$ is given in Appendix A [Eq. (A10)]. Again, $S(x,\Omega_s)$ sensitively depends on the local-oscillator phase θ. In particular, for chosen distance x the phase θ_x may be optimized in such a way that the integrated noise

$$S(x)=\int_{-\infty}^{\infty}d\Omega_s\,S(x,\Omega_s) \quad (48)$$

becomes a minimum. Note that in this case the relation $S(x)=\langle:[\Delta\hat{E}_d(x)]^2:\rangle$ is valid, with $\langle:[\Delta\hat{E}_d(x)]^2:\rangle$ from Eq. (42). To observe maximum reduction of noise in each frequency component [Eq. (A13)], the phase of the local oscillator, θ_{x,Ω_s}, must be optimized for each setting frequency Ω_s separately [Eq. (A12)].

C. Results

Since the (complex) c-number field $E(x,t)$, Eq. (21) [together with Eq. (22)], looks like the (complex) electric-field strength of a classical pulse propagating in a dispersive and absorbing dielectric, we may expect that the normally ordered electric-field strength correlation functions as given in Eq. (20) exhibit properties that bear resemblance to a number of properties of a classical pulse, such as pulse broadening and compression. However, with regard to phase-sensitive properties, such as the electric-field strength noise of squeezed pulses [Eq. (38)], we also expect that the properties actually detected sensitively depend on the phase control used. To illustrate this, let us assume that the shape function of the incoming pulse in the frequency domain, $\eta(\omega)$, is given by

$$\eta(\omega)=\eta_0 e^{-p(\omega-\omega_0)^2} \quad (49)$$

[Fig. 1(b)], where ω_0 is the center frequency and η_0 is a normalization constant defined by Eq. (23). The parameter p is a complex number, $p=p_r+ip_i$, with $p_r>0$. The real part p_r corresponds to the inverse squared spectral width and the imaginary part p_i is responsible for a frequency chirp [cf. Eq. (B11)].

1. Gaussian wave packets

To calculate the normally ordered variance of the electric-field strength observed in homodyne detection, Eq. (38), let us first consider the model of a narrow-bandwidth pulse propagating in a medium that does not give rise to higher than second-order dispersion and absorption [6], so that the (complex) wave number can approximately be given by

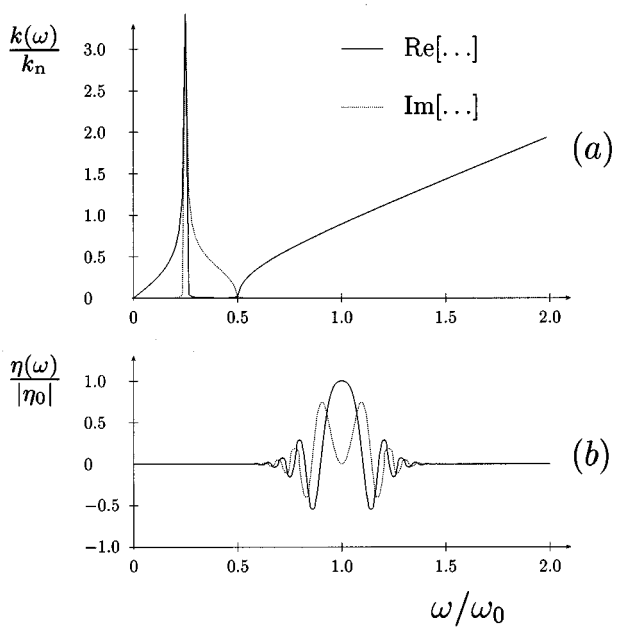

FIG. 1. The dispersion relation $k(\omega)$ based on Eq. (69) [$k_n=(\omega_0/c)\sqrt{\varepsilon_\infty}$] and the spectral shape function of the incoming pulse, $\eta(\omega)$, given in Eq. (49), are shown. The solid and dotted curves, respectively, correspond to real and imaginary parts. The following parameter values are used (Sec. III C 2): $\varepsilon_\infty=1$, $\Delta\varepsilon=3$, $\omega_r/\omega_0=2.5\times10^{-1}$, $\gamma/\omega_r=1\times10^{-3}$, $p_r\omega_0^2=3\times10^1$, $p_i\omega_0^2=-1.5\times10^2$.

$$k(\omega)=k(\omega_0+\Omega)\equiv k(\Omega)\approx k_0+k_1\Omega+\tfrac{1}{2}k_2\Omega^2, \quad (50)$$

where

$$k_j=k_{jr}+ik_{ji}\quad(j=0,1,2), \quad (51)$$

$$\Omega=\omega-\omega_0. \quad (52)$$

Using Eqs. (49) and (50) and recalling Eqs. (21), (22), and (37), and introducing the frame of reference (x,τ) moving with the group velocity k_{1r}^{-1},

$$t=k_{1r}x+\tau, \quad (53)$$

we evaluate $E_d(x,\tau)\equiv E_d(x,t=k_{1r}x+\tau)$ to obtain [Appendix B, Eqs. (B4) and (B7)]

$$E_d(x,\tau)=\frac{1}{2\pi}\int_{-\infty}^{\infty}d\Omega\,E_d(x,\Omega)e^{-i\Omega\tau}$$
$$=K_0\eta_0\sqrt{\frac{\pi}{D(x)}}\exp\left[-\frac{(\tau-ik_{1i}x)^2}{4D(x)}\right]$$
$$\times\exp[i(k_0+k_{1r}\delta\omega)x+i\delta\omega\tau], \quad (54)$$

where the abbreviations

$$\delta\omega=\omega_d-\omega_0 \quad (55)$$

and

$$D(x)=p-\tfrac{1}{2}ik_2x=D_r(x)+iD_i(x) \quad (56)$$

have been used, K_0 and η_0 being given in Eqs. (B2) and (49).

From Eqs. (38) and (39) it is clear that the observed space-time behavior of the electric-field strength variance of a pulse entering the medium in a squeezed state may resemble (dependent upon the phase control used) that of the intensity. Let us first assume that the local-oscillator phase is independent of time. We choose it according to Eq. (41), so that for given propagation length x the time-integrated variance $\langle:[\Delta\hat{E}_d(x)]^2:\rangle$, Eq. (42) together with Eq. (43), is minimal. Using Eq. (54), after some calculation we obtain

$$\langle:[\Delta\hat{E}_d(x)]^2:\rangle = 2W(x)\left\{1-\coth|s|\sqrt{\frac{D_r(x)}{|D(x)|}}\times\exp\left[-2D_r(x)\left(\delta\omega+\frac{k_{1i}x}{2D_r(x)}\right)^2\right]\right\}, \tag{57}$$

where the total-pulse intensity reads as

$$W(x)=\sqrt{\frac{2\pi^3}{D_r(x)}}|K_0|^2|\eta_0|^2\sinh^2|s|\exp\left[-2k_{0i}x+\frac{k_{1i}^2x^2}{2D_r(x)}\right] \tag{58}$$

[see Appendix B, Eqs. (B12)–(B14)]. Note that the approximation scheme only applies when the conditions

$$2k_{2i}k_{0i}>k_{1i}^2, \quad k_{0i}>0, \quad k_{2i}>0 \tag{59}$$

are satisfied, otherwise divergencies would appear. The conditions (59) obviously result from neglection of all the terms higher than second order in frequency in the expansion of the wave number, Eq. (50).

Reduction of the electric-field strength noise below the vacuum level can be observed when the second term in the curly brackets in Eq. (57) exceeds the first one, so that $\langle:[\Delta\hat{E}_d(x)]^2:\rangle<0$. It can easily be seen that $\langle:[\Delta\hat{E}_d(x)]^2:\rangle$ as a function of $\delta\omega$ attains a minimum at

$$\delta\omega=\delta\omega_x\equiv-\frac{k_{1i}x}{2D_r(x)}, \tag{60}$$

which coincides with the shift of the center frequency of the spectral function of the pulse at propagation length x [see Appendix B, Eq. (B6)]. Compensating this shift by controlling the local-oscillator frequency in such a way that (at chosen distance x) $\omega_d=\omega_0+\delta\omega_x$ is valid, we can substitute $\delta\omega_x$ for $\delta\omega$ in Eq. (57) and obtain

$$\langle:[\Delta\hat{E}_d(x)]^2:\rangle = 2W(x)\left(1-\coth|s|\sqrt{\frac{D_r(x)}{|D(x)|}}\right) \tag{61}$$

(Fig. 7). Hence, using frequency matching, reduced electric-field strength noise can be detected. Equation (61) reveals that the x region where (time-integrated) squeezing can be detected is given by the condition that

$$\left|\frac{D_i(x)}{D_r(x)}\right|<\sqrt{\coth^4|s|-1} \tag{62}$$

(Fig. 2). Recalling Eq. (56), we see that $|D_i(x)/D_r(x)|\to|k_{2r}/k_{2i}|$ when $x\to\infty$. Hence, detection of negative values of $\langle:[\Delta\hat{E}_d(x)]^2:\rangle$ at large propagation length ($x\to\infty$) requires the condition

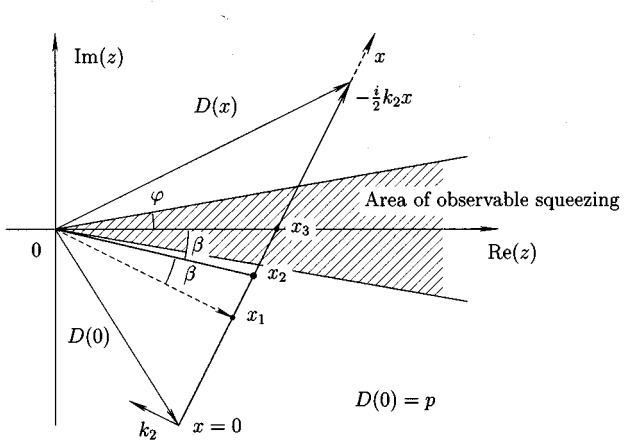

FIG. 2. The dependence on the propagation length x of the complex quantity $D(x)$ defined in Eq. (56) is shown. In the x region that corresponds to $D(x)$ inside the hatched area, with spread angle $2\varphi=2\arctan(\sqrt{\coth^4|s|-1})$, Eq. (62), the normally ordered electric-field strength variance of the overall pulse, Eq. (61), is negative. $|D(x)|$ attains a minimum when $D(x)\perp x$ ($x=x_1$ in the figure), and a minimum of the duration of the pulse, $\tau_0(x)$ [Eq. (65)], is observed at $x=x_2$.

$$\left|\frac{k_{2r}}{k_{2i}}\right|<\sqrt{\coth^4|s|-1} \tag{63}$$

to be satisfied. Clearly, in the limit when $p_i\to0$ satisfaction of the condition (63) implies that $\langle:[\Delta\hat{E}_d(x)]^2:\rangle<0$ for all values of x. Rewriting Eq. (63) as

$$|s|<s_0=\operatorname{arccoth}[(1+|k_{2r}/k_{2i}|^2)^{1/4}], \tag{64}$$

we may regard this inequality as a restriction imposed on the absolute value of s. The absolute value of s must not exceed s_0 in order to detect negative values of $\langle:[\Delta\hat{E}_d(x)]^2:\rangle$. Note that the value of s_0 decreases with increasing value of the second-order dispersion coefficient of the medium, k_{2i}, which is responsible for dephasing, but increases with the value of the second-order absorption coefficient of the medium, k_{2i}. It should be pointed out that for $|s|<s_0$ the normally ordered electric-field strength variance $\langle:[\Delta\hat{E}_d(x)]^2:\rangle$ given in Eq. (61) always evolves into negative values in the medium even when (at the entrance plane) $\langle:[\Delta\hat{E}_d(0)]^2:\rangle\geqslant0$.

Clearly, when the phase of the local oscillator is controlled in such a way that in Eq. (38) $\varphi_s+2\theta_{x,t}$ exactly compensates the phase of $E_d^2(x,t)$ at any space-time point, so that Eqs. (45) and (44) apply, the normally ordered electric-field strength variance $\langle:[\Delta\hat{E}_d(x,t)]^2:\rangle$ is always negative and fully determined by the intensity (Fig. 8). From Eqs. (39) and (54), the duration of the pulse (intensity) at propagation length x is given by

$$\tau_0(x)=\left(\frac{2|D(x)|^2}{D_r(x)}\right)^{1/2} \tag{65}$$

[cf. Eq. (94) for $\tau_0 \equiv \tau_0(0)$]. When for appropriately chosen parameters the pulse duration $\tau_0(x)$ attains at certain distance ($x = x_2$ in Fig. 2) a minimum, ordinary pulse compression is accompanied by ''compression'' of squeezing. Note that this effect can also be found in the case when the local-oscillator phase is independent of time and chosen according to Eq. (41) (Fig. 4). Needless to say, in any detection scheme the noise reduction is lost for sufficiently large values of the propagation length, because of absorption.

Let us turn to the squeezing spectrum $S(x,\Omega_s)$ defined in Eq. (46) and suppose that the local-oscillator phase is chosen in such a way that for given propagation length x and setting frequency Ω_s maximum noise reduction is observed [Eq. (A12)]. From Appendix C we obtain

$$\begin{aligned} S(x,\Omega_s) = {} & 4\pi |K_0|^2 |\eta_0|^2 \sinh^2|s| \exp[-2(k_{0i}+k_{1i}\delta\omega)x] \\ & \times \exp[-2D_r(x)(\delta\omega^2+\Omega_s^2)] \\ & \times (\cosh\{2\Omega_s[k_{1i}x+2\delta\omega D_r(x)]\} - \coth|s|) \end{aligned} \tag{66}$$

[Eq. (C5)]. We see that $S(x,\Omega_s)$ depends on the coefficients k_j only through the imaginary parts k_{ji} arising from absorption. In particular, the quadratic dependence on frequency of the imaginary part of the wave number (coefficient k_{2i}) can give rise to an x-dependent change of the width of the squeezing spectrum observed. The effect is similar to that reported in Ref. [13] for the squeezing spectrum of continuous radiation. Further, there are regions of frequency for which the noise can be enhanced and others where it can be reduced. In particular when $\delta\omega = 0$ is valid (that is to say, $\omega_d = \omega_0$), wings of enhanced noise are observed for frequencies satisfying the condition

$$|\Omega_s| > \frac{\operatorname{arccosh}(\coth|s|)}{2k_{1i}x}, \tag{67}$$

the height of the wings being proportional to $\exp[-2k_{0i}x - (2p_r + k_{2i}x)\Omega_s^2]$ (Fig. 11). The effect obviously comes from the linear dependence on frequency of the imaginary part of the wave number (coefficient k_{1i}). It is closely related to the x-dependent shift of the center frequency of the spectral function of the pulse [see Appendix B, Eq. (B6)] and quite similar to that found for $\langle{:}[\Delta\hat{E}_d(x)]^2{:}\rangle$, Eq. (57), in the case when $\omega_d = \omega_0$ ($\delta\omega = 0$). Hence, shifting the local-oscillator frequency ω_d towards $\omega_0 + \delta\omega_x$, with $\delta\omega_x$ from Eq. (60), the effect can be suppressed. In this case, Eq. (66) obviously reads as

$$\begin{aligned} S(x,\Omega_s) = {} & 4\pi |K_0|^2 |\eta_0|^2 \sinh^2|s| (1 - \coth|s|) \\ & \times \exp\left[-2k_{0i}x + \frac{k_{1i}^2 x^2}{2D_r(x)} - 2D_r(x)\Omega_s^2\right], \end{aligned} \tag{68}$$

which (for $|s| > 0$) is seen to be always negative.

2. Numerical results

The Gaussian wave-packet approximation fails when higher than second order frequency derivatives of the wave number become significant (e.g., in long-distance propagation of extremely short pulses). In this case the calculations must be performed, in general, numerically, using the actual data for the dielectric matter (and the pulse) under study. To give an example, let us consider an effectively single-resonance medium of Lorentz type whose permittivity can be given by [39]

$$\varepsilon(\omega) = \varepsilon_\infty + \frac{\omega_r^2 \Delta\varepsilon}{\omega_r^2 - \omega^2 - 2i\gamma\omega}, \tag{69}$$

where ω_r and γ, respectively, are the resonance frequency of the medium and the corresponding linewidth. Contributions to the permittivity of other resonances may be thought of as to be included in ε_∞, so that in general $\varepsilon_\infty \neq 1$. In the numerical calculation we have restricted attention to an exactly single resonance medium and assumed that $\varepsilon_\infty = 1$. The values of the other parameters in Eq. (69) and the values of the parameters of the spectral shape function of the incoming pulse, $\eta(\omega)$, given in Eq. (49) have been chosen as follows: $\Delta\varepsilon = 3$, $\omega_r/\omega_0 = 2.5\times10^{-1}$, $\gamma/\omega_r = 1\times10^{-3}$, $p_r\omega_0^2 = 3\times10^1$, $p_i\omega_0^2 = -1.5\times10^2$. The resulting dependence on frequency of the wave number, $k(\omega)$, can then be found from Eq. (7) together with Eqs. (6) and (69) [Fig. 1(a)]. The function $\eta(\omega)$ spectrally extends over a relatively large region where $k_r''(\omega) < 0$ [Fig. 1(b)]. The numerical results are compared with those obtained in the Gaussian wave-packet approximation, using $k(\omega)$ according to Eq. (69) and making in Eq. (50) the identifications

$$k_0 = k(\omega_0), \quad k_1 = k'(\omega)|_{\omega=\omega_0}, \quad k_2 = k''(\omega)|_{\omega=\omega_0}, \tag{70}$$

which particularly implies that the value of s_0 in the inequality (64) is given by $s_0 = 8.2\times10^{-2}$.

In the figures, (x,τ) refer to a moving reference frame [Eq. (53)]. The values of x and τ, respectively, are given in units of the initial-pulse duration $\tau_0 \equiv \tau_0(=0) = (2|p|^2/p_r)^{1/2}$ [cf. Eqs. (65) and (B10)] and the dispersion length $L_d = \tau_0^2/|k_2|$, see, e.g., [6]. In Fig. 3 the evolution of the pulse intensity given in Eq. (39) [$I_d(x,\tau) \equiv I_d(x, t = k_{1r}x + \tau)$] is shown. The evolution of the observed normally ordered electric-field strength variance given in Eq. (38) [$\langle{:}[\Delta\hat{E}_d(x,\tau)]^2{:}\rangle \equiv \langle{:}[\Delta\hat{E}_d(x, t = k_{1r}x+\tau)]^2{:}\rangle$] is shown in Fig. 4 for the case when the local-oscillator phase is independent of time and chosen according to Eq. (41). The ''compression'' of squeezing in Fig. 4 corresponds to the compression of the pulse intensity in Fig. 3. Restricting attention to a time-independent local-oscillator phase θ_x, from Sec. III B we know that choosing θ_x according to Eq. (41) ensures observation of maximum noise reduction in the sense that the time-integrated normally ordered variance $\langle{:}[\Delta\hat{E}_d(x)]^2{:}\rangle$ is minimal. In Figs. 6 and 7, respectively, the so-optimized θ_x, Eq. (41), and the resulting $\langle{:}[\Delta\hat{E}_d(x)]^2{:}\rangle$, Eq. (42), are shown as functions of the propagation length x. Note that θ_x does not depend on the absolute value of squeezing parameter s. From Fig. 7 we see that, in agreement with the Gaussian wave-packet approximation, $\langle{:}[\Delta\hat{E}_d(x)]^2{:}\rangle$ is negative in the whole x region, provided that $|s| < s_0$ (strong second-order absorption). We

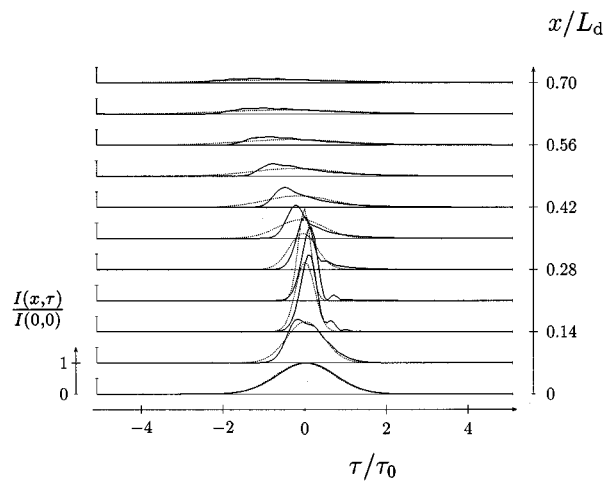

FIG. 3. The pulse intensity $I_d(x,\tau)$, Eq. (39), is shown as a function of τ for various values of the propagation length x, where $\tau_0=(2|p|^2/p_r)^{1/2}$ and $L_d=\tau_0^2/|k_2|$. The values of the pulse and medium parameters are given in Fig. 1. The dotted curves correspond to the Gaussian wave-packet approximation, Sec. III C 1.

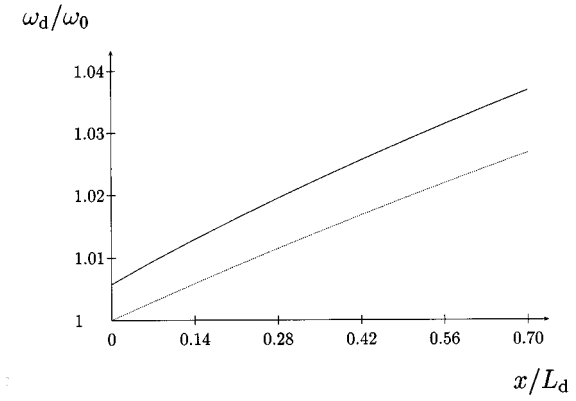

FIG. 5. The local-oscillator frequency ω_d required for frequency matching is shown as a function of the propagation length x; $\omega_d=\omega_0+\delta\omega_x$, with $\delta\omega_x$ from Eq. (71) or, in the Gaussian wave-packet approximation, from Eq. (60). The values of the pulse and medium parameters are given in Fig. 1. The dotted curve corresponds to the Gaussian wave-packet approximation, Sec. III C 1.

further see that in the case when $|s|>s_0$ (weak second-order absorption) the region where negative values of $\langle:[\Delta\hat{E}_d(x)]^2:\rangle$ can be observed is limited: $\langle:[\Delta\hat{E}_d(x)]^2:\rangle$ starts from positive values at $x=0$, evolves into negative values with increasing x, and attains again positive values in the further course of pulse propagation. In the Gaussian wave-packet approximation the region of negative values of $\langle:[\Delta\hat{E}_d(x)]^2:\rangle$ is limited by the hatched area in Fig. 2. Comparing Figs. 6 and 7 we see that observation of maximum noise reduction requires careful phase control, because in the vicinity of the minimum of $\langle:[\Delta\hat{E}_d(x)]^2:\rangle$ the phase θ_x sensitively depends on x.

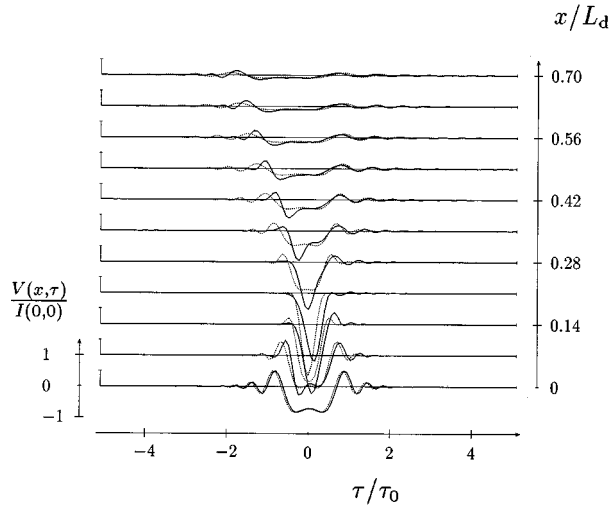

FIG. 4. The normally ordered electric-field strength variance $\langle:[\Delta\hat{E}_d(x,\tau)]^2:\rangle$, Eq. (38) together with Eq. (39), is shown as a function of τ for various values of the propagation length x, and $|s|=8\times10^{-2}$, where $V(x,\tau)=\langle:[\Delta\hat{E}_d(x,\tau)]^2:\rangle/(2\coth|s|)$, $\tau_0=(2|p|^2/p_r)^{1/2}$, and $L_d=\tau_0^2/|k_2|$. The local-oscillator frequency and phase are chosen according to Figs. 5 and 6(a), respectively. The values of the pulse and medium parameters are given in Fig. 1. The dotted curves correspond to the Gaussian wave-packet approximation, Sec. III C 1.

In Figs. 4 and 7 frequency matching is assumed, that is to say, for chosen propagation length x the optimal value of the local-oscillator frequency ω_d given by $\omega_d=\omega_0+\delta\omega_x$ is used, where

$$\delta\omega_x=\frac{\int d\Omega\,\Omega|E_d(x,\Omega)|}{\int d\Omega|E_d(x,\Omega)|}, \tag{71}$$

$E_d(x,\Omega)$ being the Fourier transform of $E_d(x,\tau)$ [cf. Eq. (B4)]. Note that in the Gaussian wave-packet approximation Eq. (71) reduces to Eq. (60). An example for the dependence on x of $\delta\omega_x$ is given in Fig. 5. According to Eq. (41) [together with Eqs. (37), (21), and (22)] the phase θ_x depends on the chosen local-oscillator frequency. The effect of frequency matching on the phase θ_x is illustrated in Fig. 6.

Appropriate local-oscillator phase control at any space-time point would of course enable one to observe always negative values of $\langle:[\Delta\hat{E}_d(x,t)]^2:\rangle$. As already mentioned, when the phase $\varphi_s+2\theta_{x,t}$ exactly compensates the phase of $E_d^2(x,t)$ [Eq. (44)], then the minimum noise is observed and Eq. (45) applies (Fig. 8). In this case the evolution of $\langle:[\Delta\hat{E}_d(x,t)]^2:\rangle$ in space and time is fully determined by that of the intensity. In particular, there is a one-to-one correspondence between classical pulse compression and compression of the electric-field strength noise. In this region substantially enhanced squeezing can be observed. Figure 8 also illustrates the limits of application of the Gaussian wave-packet approximation. The asymmetries and substructures in the pulse profile obviously arise from higher than second-order terms in the expansion of the complex wave number, which are omitted in the Gaussian wave-packet approximation.

In Fig. 9 the squeezing spectrum $S(x,\Omega_s)$, Eq. (A10), is shown for the case when the local-oscillator frequency and phase, respectively, are chosen according to Eqs. (71) and (41) [Figs. 5 and 6(a)]. The situation corresponds to that in

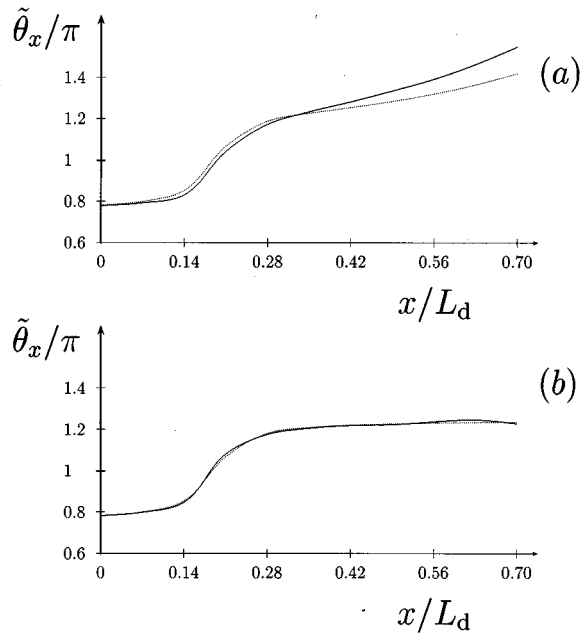

FIG. 6. The local-oscillator phase θ_x, Eq. (41), yielding the time-integrated normally ordered electric-field strength variance $\langle:[\Delta\hat{E}_d(x)]^2:\rangle$, Eq. (42) together with Eq. (43), is shown as a function of the propagation length x, where $\tilde{\theta}_x=2[\theta_x+(k_{0r}+\delta\omega k_{1r})x]$ and $L_d=\tau_0^2/|k_2|$. (a) $\omega_d=\omega_0+\delta\omega_x$, with $\delta\omega_x$ from Eq. (71) or, in the Gaussian wave-packet approximation, from Eq. (60) (Fig. 5). (b) $\omega_d=\omega_0$. The values of the pulse and medium parameters are given in Fig. 1. The dotted curves correspond to the Gaussian wave-packet approximation, Sec. III C 1.

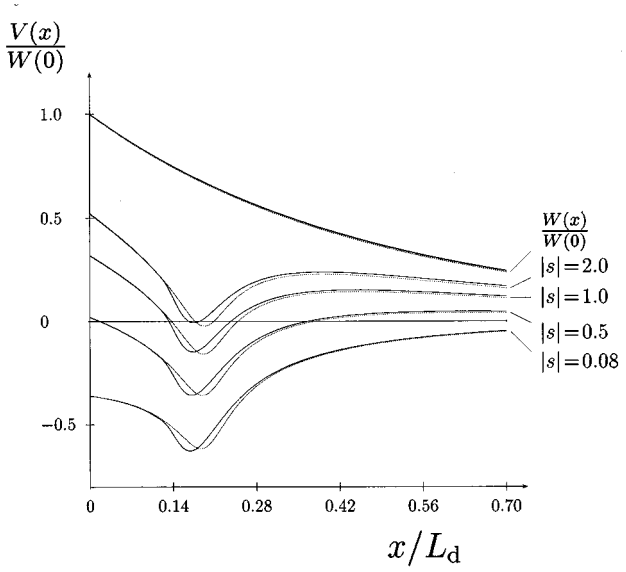

FIG. 7. The time-integrated intensity $W(x)$, Eq. (43), and the time-integrated normally ordered electric-field strength variance $\langle:[\Delta\hat{E}_d(x)]^2:\rangle$, Eq. (42) together with Eq. (43), for different absolute values of the squeezing parameter s are shown as functions of the propagation length x, where $V(x)=\langle:[\Delta\hat{E}_d(x)]^2:\rangle/(2\coth|s|)$ and $L_d=\tau_0^2/|k_2|$. The local-oscillator frequency and phase are chosen according to Figs. 5 and 6(a), respectively. The values of the pulse and medium parameters are given in Fig. 1. The dotted curves correspond to the Gaussian wave-packet approximation, Sec. III C 1.

Fig. 4. Owing to the choice of the local-oscillator phase, integration of $S(x,\Omega_s)$ over all frequencies yields the time-integrated normally ordered electric-field strength correlation function $\langle:[\Delta\hat{E}_d(x)]^2:\rangle$ shown in Fig. 7. From inspection of Fig. 9 we see that only in the x region in which maximum noise reduction can be observed are nearly all the frequency components (that are relevant for the pulse) squeezed. For fixed local-oscillator phase, such a uniform behavior of the frequency components is of course not possible in an extended x region, because of dispersion-assisted dephasing. Optimizing the local-oscillator phase for each frequency component separately [Eq. (A12)] enables one to suppress this dephasing and at any space-time point maximum noise reduction can be observed (Fig. 10).

The effect of frequency detuning between local oscillator and pulse is demonstrated in Fig. 11. As already mentioned, owing to frequency-dependent absorption an x-dependent shift of the center frequency of the spectral function of the pulse is observed. Hence, tuning the local-oscillator frequency to the center frequency of the incoming pulse, in the further course of pulse propagation detuning necessarily appears. The enhanced noise observed in this case (the wings in Fig. 11) can be suppressed in a detection scheme, where frequency matching is used, so that at chosen propagation length x the local oscillator-frequency equals the actual center frequency of the spectral function of the pulse (Fig. 10).

IV. SUMMARY AND CONCLUSIONS

In this paper we have considered the propagation of short quantum light pulses in dispersive and absorbing linear di-

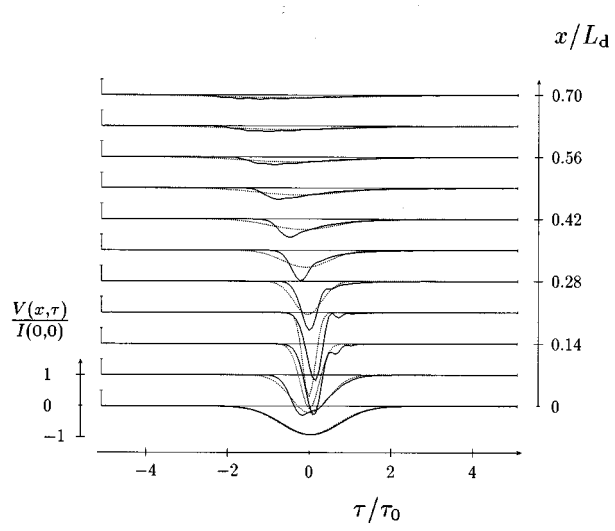

FIG. 8. The normally ordered electric-field strength variance $\langle:[\Delta\hat{E}_d(x,\tau)]^2:\rangle$, Eq. (45), is shown as a function of τ for various values of the propagation length x, and $|s|=8\times10^{-2}$, where $V(x,\tau)=\langle:[\Delta\hat{E}_d(x,\tau)]^2:\rangle/(2\coth|s|)$, $\tau_0=(2|p|^2/p_r)^{1/2}$, and $L_d=\tau_0^2/|k_2|$. The phase of the local oscillator, $\theta_{x,t}$, is chosen in such a way that in Eq. (38) $\varphi_s+2\theta_{x,t}$ exactly compensates the phase of $E_d^2(x,t)$ [Eq. (44)], and in any space-time point the minimum noise is observed. The values of the pulse and medium parameters are given in Fig. 1. The dotted curves correspond to the Gaussian wave-packet approximation, Sec. III C 1.

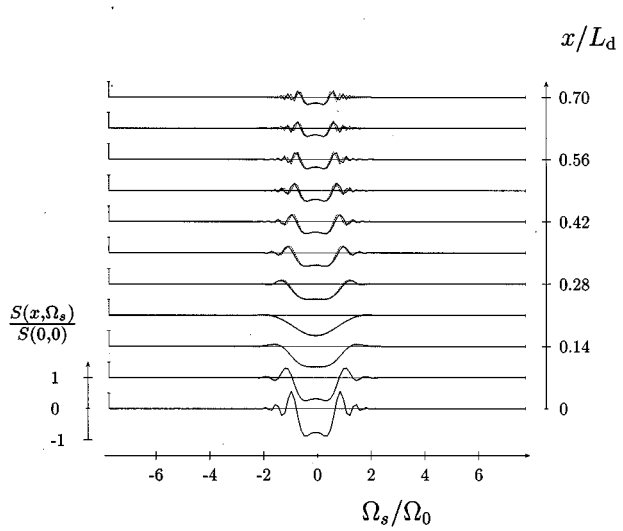

FIG. 9. The squeezing spectrum $S(x,\Omega_s)$, Eq. (A10), is shown for various values of the propagation length x, and $|s|=8\times10^{-2}$, where $\Omega_0=(2p_r)^{-1/2}$ and $L_d=\tau_0^2/|k_2|$. The local-oscillator frequency and phase are chosen according to Figs. 5 and 6(a), respectively. The values of the pulse and medium parameters are given in Fig. 1. The dotted curves correspond to the Gaussian wave-packet approximation, Sec. III C 1.

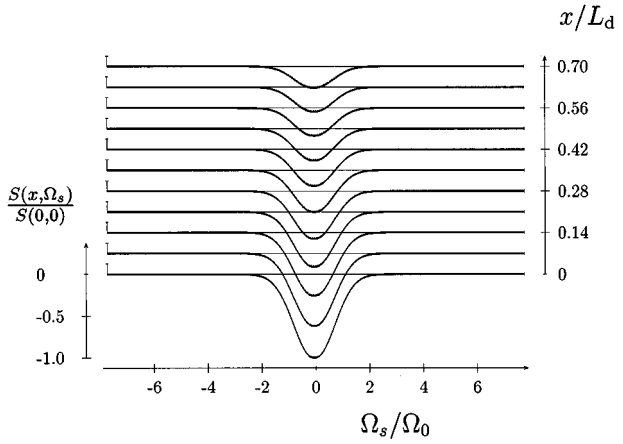

FIG. 10. The squeezing spectrum $S(x,\Omega_s)$, Eq. (A13), is shown for various values of the propagation length x, where $\Omega_0=(2p_r)^{-1/2}$ and $L_d=\tau_0^2/|k_2|$. Frequency matching is considered (Fig. 5) and the local-oscillator phase is chosen according to Eq. (A12), so that at any space-frequency point minimum noise is observed. Note that in this case $S(x,\Omega_s)/S(0,0)$ is independent of $|s|$. The values of the pulse and medium parameters are given in Fig. 1. The dotted curves correspond to the Gaussian wave-packet approximation, Sec. III C 1.

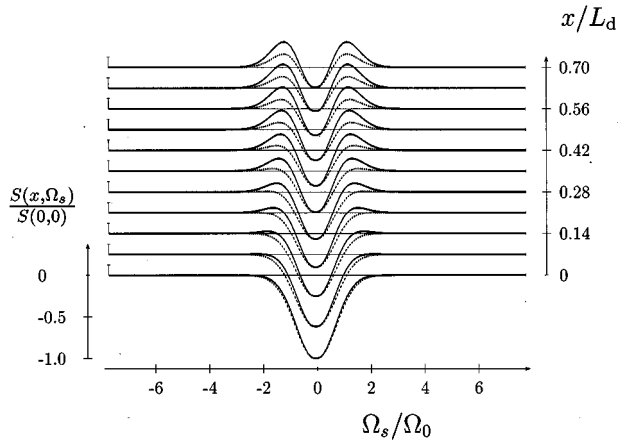

FIG. 11. The squeezing spectrum $S(x,\Omega_s)$, Eq. (A13), is shown for various values of the propagation length x, and $|s|=2$, where $\Omega_0=(2p_r)^{-1/2}$ and $L_d=\tau_0^2/|k_2|$. The local-oscillator phase is chosen according to Eq. (A12), so that at any space-frequency point minimum noise is observed, however without frequency matching ($\omega_d=\omega_0$). The values of the pulse and medium parameters are given in Fig. 1. The dotted curves correspond to the Gaussian wave-packet approximation, Sec. III C 1.

electrics that are not thermally excited in the optical frequency region of the pulses. The space-time evolution of the quantum-statistical properties of the pulses has been described in terms of normally ordered correlation functions of the electric-field strength, which can be expressed in terms of normally ordered moments of the photonic creation and destruction operators associated with the nonmonochromatic modes of the pulses at the entrance plane. The theory has been applied to single-mode pulses that enter the medium in a squeezed vacuum state. The development of the normally ordered electric-field strength variance in the further course of pulse propagation has been studied in both the time and frequency domains, with special emphasis on homodyne detection. It has been shown that owing to the dependence on frequency of the complex wave number determining dispersion and absorption the result of detection can sensitively depend on the local-oscillator phase and frequency control.

Using a model permittivity that is based on a single medium resonance of Lorentz type and assuming for the incoming pulse a Gaussian spectral shape function, both analytical and numerical results have been presented in order to analyze the effects of dispersion and absorption on the electric-field strength noise observed in homodyne detection. A number of effects, such as pulse broadening and compression, well known from classical optics have been shown to be also observable with regard to the electric-field strength noise. In particular, ordinary pulse compression can be accompanied by ''compression'' of squeezing, so that enhanced squeezing can be observed, the compression distance coinciding with the classical one.

When the local-oscillator phase is time independent (that is to say, it does not vary with time on a time scale given by the duration of the pulse under consideration), the optimal phase for detection of squeezing can be determined from the requirement that the total electric-field strength noise detected is minimal. The so-optimized phase varies with the length of propagation of the pulse in the medium. In this scheme, the region of propagation length in which total-pulse squeezing can be observed is limited, in general, by an upper and lower boundary and decreases with increasing strength of squeezing of the incoming pulse. In particular, long-distance detection of total-pulse squeezing is, in general, not possible. Only in the case when the absolute value of the squeezing parameter of the incoming pulse does not exceed a

critical value can squeezing be detected, without restriction of the length of propagation. The critical value is determined by two rival effects. Dispersion tries to decrease it, because of dephasing, whereas frequency-dependent (higher-order) absorption has the tendency to enlarge it, since it selectively removes sideband components from the pulse which are then missing in the dephasing process. On the other hand, frequency-dependent absorption has also the tendency to shift the center frequency of the spectral function of the pulse during propagation in the medium. In this case, detection of maximum noise reduction requires the local-oscillator frequency to be tuned to the center frequency of the pulse at a chosen length of propagation in the medium.

It should be noted that effects that may arise from input–output couplings have been ignored throughout the paper. Their inclusion in the theory requires consideration of the boundary conditions at the surfaces of discontinuity (entrance and exit planes) and can be performed by applying the correct input-output relations given in Ref. [40] in place of Eq. (9). As a consequence of using modified input-output relations, a spectral function of the pulse, $E(x,\omega)$, is obtained that may differ from that in Eq. (22). Clearly, knowing the spectral function, all the calculations may be performed in a similar way as in this paper.

ACKNOWLEDGMENTS

This work was supported by the Deutsche Forschungsgemeinschaft. We are grateful to T. Gruner for valuable discussions.

APPENDIX A: SQUEEZING SPECTRUM

Using Eqs. (36) and (4), we find that

$$\hat{E}_d(x,t)=\int_0^\infty d\omega\, K(\omega)e^{ik(\omega)x}e^{-i(\omega-\omega_d)t+i\theta}\hat{a}(\omega)+\text{H.c.}, \tag{A1}$$

so that Eq. (47) takes the form

$$\begin{aligned}\hat{E}_d(x,\Omega_s)=\int_{-\infty}^{\infty}dt\, e^{i\Omega_s t}\hat{E}_d(x,t)=2\pi\int_0^\infty d\omega\\ \times[K(\omega)e^{ik(\omega)x+i\theta}\delta(-\omega+\omega_d+\Omega_s)\hat{a}(\omega)\\ +K^*(\omega)e^{-ik^*(\omega)x-i\theta}\delta(\omega-\omega_d+\Omega_s)\hat{a}^\dagger(\omega)],\end{aligned} \tag{A2}$$

where

$$\begin{aligned}\hat{E}_d(x,\Omega_s)=2\pi[K_+(\Omega_s)e^{ik_+(\Omega_s)x+i\theta}\hat{a}(\omega_d+\Omega_s)\\ +K_-^*(\Omega_s)e^{-ik_-^*(\Omega_s)x-i\theta}\hat{a}^\dagger(\omega_d-\Omega_s)],\end{aligned} \tag{A3}$$

with

$$K_\pm(\Omega_s)=\Theta(\omega_d\pm\Omega_s)K(\omega_d\pm\Omega_s), \tag{A4}$$

$$k_\pm(\Omega_s)=k(\omega_d\pm\Omega_s) \tag{A5}$$

[$\Theta(x)$, unit step function]. We now calculate $S(x,\Omega_s)$ defined by Eq. (46). From the above we obtain

$$\begin{aligned}S(x,\Omega_s)&=\frac{1}{2\pi}\langle{:}\Delta\hat{E}_d(x,\Omega_s)\Delta\hat{E}_d(x,-\Omega_s){:}\rangle\\ &=2\pi(K_+(\Omega_s)K_-(\Omega_s)\exp\{i[k_+(\Omega_s)+k_-(\Omega_s)]x+2i\theta\}\langle\Delta\hat{a}(\omega_d+\Omega_s)\Delta\hat{a}(\omega_d-\Omega_s)\rangle\\ &\quad+K_+^*(\Omega_s)K_-^*(\Omega_s)\exp\{-i[k_+^*(\Omega_s)+k_-^*(\Omega_s)]x-2i\theta\}\langle\Delta\hat{a}^\dagger(\omega_d+\Omega_s)\Delta\hat{a}^\dagger(\omega_d-\Omega_s)\rangle\\ &\quad+|K_+(\Omega_s)|^2e^{-2\gamma_+(\Omega_s)x}\langle\Delta\hat{a}^\dagger(\omega_d+\Omega_s)\Delta\hat{a}(\omega_d+\Omega_s)\rangle+|K_-(\Omega_s)|^2e^{-2\gamma_-(\Omega_s)x}\langle\Delta\hat{a}^\dagger(\omega_d-\Omega_s)\Delta\hat{a}(\omega_d-\Omega_s)\rangle),\end{aligned} \tag{A6}$$

where

$$\gamma_\pm(\Omega_s)=\text{Im}\{k_\pm(\Omega_s)\}. \tag{A7}$$

Recalling Eqs. (19), (31), and (32), we obtain

$$\langle\Delta\hat{a}(\omega)\Delta\hat{a}(\omega')\rangle=-\eta(\omega)\eta(\omega')e^{i\varphi_s}\cosh|s|\sinh|s|, \tag{A8}$$

$$\langle\Delta\hat{a}^\dagger(\omega)\Delta\hat{a}(\omega')\rangle=\eta^*(\omega)\eta(\omega')\sinh^2|s|. \tag{A9}$$

Finally, combining Eqs. (A6), (A8), and (A9) yields

$$\begin{aligned}S(x,\Omega_s)=2\pi[|K_+(\Omega_s)|^2|\eta_+(\Omega_s)|^2e^{-2\gamma_+(\Omega_s)x}+|K_-(\Omega_s)|^2|\eta_-(\Omega_s)|^2e^{-2\gamma_-(\Omega_s)x}]\sinh^2|s|\\ -4\pi\,\text{Re}(K_+(\Omega_s)\eta_+(\Omega_s)K_-(\Omega_s)\eta_-(\Omega_s)\exp\{i[k_+(\Omega_s)+k_-(\Omega_s)]x+i(\varphi_s+2\theta)\})\cosh|s|\sinh|s|,\end{aligned} \tag{A10}$$

where

$$\eta_\pm(\Omega_s)=\eta(\omega_d\pm\Omega_s). \tag{A11}$$

When the phase θ_{x,Ω_s} is chosen to minimize $S(x,\Omega_s)$ at any space-frequency point,

$$\varphi_s + 2\theta_{x,\Omega_s} = -\arg(K_+(\Omega_s)\eta_+(\Omega_s)K_-(\Omega_s)\eta_-(\Omega_s)\exp\{i[k_+(\Omega_s)+k_-(\Omega_s)]x\}), \tag{A12}$$

then Eq. (A10) reduces to

$$S(x,\Omega_s) = 2\pi[|K_+(\Omega_s)|^2|\eta_+(\Omega_s)|^2 e^{-2\gamma_+(\Omega_s)x} + |K_-(\Omega_s)|^2|\eta_-(\Omega_s)|^2 e^{-2\gamma_-(\Omega_s)x}]\sinh^2|s| - 4\pi|K_+(\Omega_s)\eta_+(\Omega_s)K_-(\Omega_s)\eta_-(\Omega_s)|\exp\{-[\gamma_+(\Omega_s)+\gamma_-(\Omega_s)]x\}\cosh|s|\sinh|s|. \tag{A13}$$

APPENDIX B: PROOF OF EQ. (57)

Using Eqs. (21), (22), and (37), we may write

$$E_d(x,t) = e^{i\omega_d t}\int_0^\infty d\omega\, K(\omega)\,\eta(\omega)\exp[ik(\omega)x - i\omega t] = \int_{-\omega_0}^\infty d\Omega\, K(\omega_0+\Omega)\,\eta(\omega_0+\Omega)\exp[ik(\omega_0+\Omega)x - i(\Omega-\delta\omega)t], \tag{B1}$$

where $\delta\omega = \omega_d - \omega_0$, Eq. (55). Recalling Eqs. (49) and (50), assuming

$$K(\omega_0+\Omega) \approx K(\omega_0) \equiv K_0, \tag{B2}$$

and extending the Ω integral to $-\infty$, from Eq. (B1) we obtain

$$E_d(x,t) = K_0\eta_0 e^{ik_0x}\int_{-\infty}^\infty d\Omega \exp\left[-p\Omega^2 + i\left(k_1\Omega + \frac{1}{2}k_2\Omega^2\right)x - i(\Omega-\delta\omega)t\right], \tag{B3}$$

which may be rewritten as, on using Eq. (53) [$E_d(x,\tau) \equiv E_d(x,t=k_{1r}x+\tau)$],

$$E_d(x,\tau) = \frac{1}{2\pi}\int_{-\infty}^\infty d\Omega\, E_d(x,\Omega)e^{-i\Omega\tau}, \tag{B4}$$

where

$$E_d(x,\Omega) = 2\pi K_0\eta_0\exp[i(k_0+\delta\omega k_{1r})x] \times \exp[-k_{1i}(\Omega+\delta\omega)x - (p - \tfrac{1}{2}ik_2x)(\Omega+\delta\omega)^2]. \tag{B5}$$

From Eq. (B5) the absolute value of $E_d(x,\Omega)$ is easily seen to attain the maximum at (the center frequency)

$$\Omega = \delta\omega_x - \delta\omega, \tag{B6}$$

with $\delta\omega_x$ from Eq. (60), which reveals that the center frequency of the spectral function of the pulse, Eq. (22), is shifted towards $\omega_0 + \delta\omega_x$, because of the dependence on frequency of the absorption. Evaluating the integral in Eq. (B4) yields

$$E_d(x,\tau) = K_0\eta_0\sqrt{\frac{\pi}{D(x)}}\exp\left[-\frac{(\tau - ik_{1i}x)^2}{4D(x)}\right] \times \exp[i(k_0+\delta\omega k_{1r})x + i\delta\omega\tau], \tag{B7}$$

with $D(x)$ from Eq. (56), and hence

$$|E_d(x,\tau)|^2 = \frac{\pi|K_0|^2|\eta_0|^2}{|D(x)|}\exp[-2k_{0i}x] \times \exp\left[-\frac{\tau^2 D_r(x) - 2\tau D_i(x)k_{1i}x - D_r(x)k_{1i}^2x^2}{2|D(x)|^2}\right]. \tag{B8}$$

In particular, for $x=0$ (entrance plane) from Eq. (B7) we find that

$$E_d(0,\tau) \sim \exp\left[-\frac{\tau^2}{2}\left(\frac{1}{\tau_0^2} + i\alpha\right)\right], \tag{B9}$$

where

$$\tau_0 = \left(\frac{2|p|^2}{p_r}\right)^{1/2} \tag{B10}$$

and

$$\alpha = -\frac{p_i}{2|p|^2}, \tag{B11}$$

respectively, are the duration and chirp of the incoming pulse.

We evaluate $\int_{-\infty}^\infty d\tau\, E_d^2(x,\tau)$ to obtain

$$\int_{-\infty}^\infty d\tau E_d^2(x,\tau) = \pi K_0^2\eta_0^2\sqrt{\frac{2\pi}{D(x)}} \times \exp[2i(k_0+\delta\omega k_1)x - 2\delta\omega^2 D(x)], \tag{B12}$$

so that Eq. (41) takes the form

$$\varphi_s + 2\theta_x = \arg\left[\frac{\sqrt{D(x)}}{K_0^2 \eta_0^2}\right] - 2(k_{0r} + \delta\omega k_{1r})x + 2(\delta\omega)^2 D_i(x). \tag{B13}$$

Evaluating the integral $\int_{-\infty}^{\infty} d\tau\, |E_d(x,\tau)|^2$ yields

$$\int_{-\infty}^{\infty} d\tau |E_d(x,\tau)|^2 = \pi |K_0|^2 |\eta_0|^2 \sqrt{\frac{2\pi}{D_r(x)}} \times \exp\left[-2k_{0i}x + \frac{k_{1i}^2 x^2}{2D_r(x)}\right]. \tag{B14}$$

Combining Eqs. (42), (43), (B12), and (B14), we finally arrive at Eq. (57) [together with Eq. (58)].

APPENDIX C: PROOF OF EQ. (66)

To apply Eq. (A13) to Gaussian wave packets considered in Appendix B, we first recall Eqs. (B2) and (49), so that Eqs. (A4) and (A11) read as

$$K_{\pm}(\Omega_s) = K_0, \tag{C1}$$

$$\eta_{\pm}(\Omega_s) = \eta_0 \exp[-p(\delta\omega \pm \Omega_s)^2] \tag{C2}$$

[$\delta\omega = \omega_d - \omega_0$, Eq. (55)]. Next, Eq. (A7) together with Eq. (A5),

$$\gamma_{\pm}(\Omega_s) = \mathrm{Im}\{k_{\pm}(\Omega_s)\} = \mathrm{Im}\{k(\omega_0 + \delta\omega \pm \Omega_s)\}, \tag{C3}$$

may be rewritten as, on using Eq. (50),

$$\gamma_{\pm}(\Omega_s) = k_{0i} + k_{1i}(\delta\omega \pm \Omega_s) + \tfrac{1}{2}k_{2i}(\delta\omega \pm \Omega_s)^2. \tag{C4}$$

Finally, using Eqs. (C1), (C2), and (C4), from Eq. (A13) we find that

$$S(x,\Omega_s) = 4\pi |K_0|^2 |\eta_0|^2 \sinh^2|s| \exp[-2(k_{0i} + k_{1i}\delta\omega)x] \times \exp[-2D_r(x)(\delta\omega^2 + \Omega_s^2)] \times (\cosh\{2\Omega_s[k_{1i}x + 2\delta\omega D_r(x)]\} - \coth|s|), \tag{C5}$$

where, according to Eq. (56),

$$D_r(x) = p_r + \tfrac{1}{2}k_{2i}x. \tag{C6}$$

[1] E. Yablonovitch and K.M. Leung, Physica **175B**, 81 (1991).
[2] R.Y. Chiao, Phys. Rev. A **48**, R34 (1993).
[3] R.Y. Chiao, P.G. Kwiat, and A.M. Steinberg, Quantum Semiclass. Opt. **7**, 259 (1995).
[4] A.M. Steinberg and R.Y. Chiao, Phys. Rev. A **51**, 3525 (1995).
[5] M.J. Adams and I.D. Henning, *Optical Fibres and Sources for Communications* (Plenum Press, New York, 1990).
[6] S.A. Akhmanov, V.A. Vysloukh, and A.S. Chirkin, *Optics of Femtosecond Laser Pulses* (American Institute of Physics, New York, 1992).
[7] W. Vogel and D.-G. Welsch, *Lectures on Quantum Optics* (Akademie Verlag, Berlin/VCH Publishers, New York, 1994).
[8] J.D. Franson, Phys. Rev. A **45**, 3126 (1992).
[9] A.M. Steinberg, P.G. Kwiat, and R.Y. Chiao, Phys. Rev. Lett. **68**, 2421 (1992).
[10] A.M. Steinberg, P.G. Kwiat, and R.Y. Chiao, Phys. Rev. A **45**, 6659 (1992).
[11] J. Jeffers and S.M. Barnett, Phys. Rev. A **47**, 3291 (1993).
[12] S.M. Barnett, B. Huttner, and R. Loudon, Phys. Rev. Lett. **68**, 3698 (1992).
[13] J. Jeffers and S.M. Barnett, J. Mod. Opt. **41**, 1121 (1994).
[14] Y. Lai and H.A. Haus, Phys. Rev. A **40**, 844 (1989); **40**, 854 (1989).
[15] P.D. Drummond and S.J. Carter, J. Opt. Soc. Am. B **4**, 1565 (1987).
[16] H.A. Haus and Y. Lai, J. Opt. Soc. Am. B **7**, 386 (1990).
[17] P.Q. Drummond, R.M. Shelby, S.R. Friberg, and Y. Yamamoto, Nature **365**, 307 (1993).
[18] L. Knöll, W. Vogel, and D.-G. Welsch, Phys. Rev. A **36**, 3803 (1987); also see Ref. [7].
[19] R.J. Glauber and M. Lewenstein, Phys. Rev. A **43**, 467 (1991).
[20] H. Khosravi and R. Loudon, Proc. R. Soc. London Ser. A **433**, 337 (1991); **436**, 373 (1992).
[21] P.D. Drummond, Phys. Rev. A **42**, 6845 (1990).
[22] B. Huttner, J.J. Baumberg, and S.M. Barnett, Europhys. Lett. **16**, 177 (1991).
[23] P.W. Milonni, J. Mod. Opt. **42**, 1991 (1995).
[24] J. Abram and E. Cohen, Phys. Rev. A **44**, 500 (1991).
[25] G.S. Agarwal, Phys. Rev. A **11**, 230 (1975).
[26] M. Fleischhauer and M. Schubert, J. Mod. Opt. **38**, 677 (1991).
[27] B. Huttner and S.M. Barnett, Europhys. Lett. **18**, 487 (1992); Phys. Rev. A **46**, 4306 (1992).
[28] L. Knöll and U. Leonhardt, J. Mod. Opt. **39**, 1253 (1992).
[29] D. Kupiszewska, Phys. Rev. A **46**, 2286 (1992).
[30] S.-T. Ho and P. Kumar, J. Opt. Soc. Am. B **10**, 1620 (1993).
[31] J.R. Jeffers, N. Imoto, and R. Loudon, Phys. Rev. A **47**, 3346 (1993).
[32] T. Gruner and D.-G. Welsch, Phys. Rev. A **51**, 3246 (1995).
[33] S.M. Barnett, R. Matloob, and R. Loudon, J. Mod. Opt. **42**, 1165 (1995).
[34] T. Gruner and D.-G. Welsch, Phys. Rev. A **53**, 1818 (1996).
[35] U.M. Titulaer and R.J. Glauber, Phys. Rev. **145**, 1041 (1966).
[36] K.J. Blow, R. Loudon, S.J.D. Phoenix, and T.J. Shepherd, Phys. Rev. A **42**, 4102 (1990).
[37] D.F. Walls and G.J. Milburn, *Quantum Optics* (Springer-Verlag, Berlin, 1994).
[38] W. Vogel, Phys. Rev. Lett. **67**, 2450 (1991); Phys. Rev. A **51**, 4160 (1995).
[39] R. Loudon, J. Phys. A **3**, 233 (1970).
[40] T. Gruner and D.-G. Welsch, Phys. Rev. A (to be published).